Boosting the Quantitative Inorganic Surface-Enhanced Raman Scattering Sensing to the Limit: The Case of Nitrite/Nitrate Detection

Miguel A. Correa-Duarte,*[†] Nicolas Pazos Perez,[‡,§] Luca Guerrini,[‡,§] Vincenzo Giannini,[||] and Ramon A. Alvarez-Puebla*[‡,§,⊥]

[†]Departamento de Química Física, Biomedical Research Center (CINBIO) and Institute of Biomedical Research of Vigo (IBIV), Universidade de Vigo, 36310 Vigo, Spain

[‡]Departamento de Química Física e Inorgánica, Universitat Rovira i Virgili and Centro Tecnologico de la Quimica de Cataluña, Carrer de Marcel·lí Domingo s/n, 43007 Tarragona, Spain
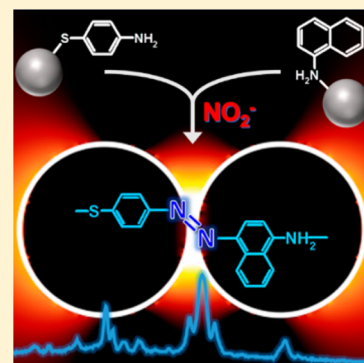
[§]Medcom Advance SA, Viladecans Bussines Park, Carrer de Bertran i Musitu, 83—85, 08840 Viladecans (Barcelona), Spain

[||]Department of Physics, Imperial College, London SW7 2AZ, U.K.

[⊥]ICREA, Passeig Lluís Companys 23, 08010 Barcelona, Spain

Ⓢ *Supporting Information*

ABSTRACT: A high-performance ionic-sensing platform has been developed by an interdisciplinary approach, combining the classical colorimetric Griess reaction and new concepts of nanotechnology, such as plasmonic coupling of nanoparticles and surface-enhanced Raman scattering (SERS) spectroscopy. This approach exploits the advantages of combined SERS/surface-enhanced resonant Raman Scattering (SERRS) by inducing the formation of homogeneous hot spots and a colored complex in resonance with the laser line, to yield detection limits for nitrite down to the subpicomolar level. The performance of this new method was compared with the classical Griess reaction and ionic chromatography showing detection limits about 6 and 3 orders of magnitude lower, respectively.

Ionic inorganic species are essential for sustaining all forms of life, but excess in their concentration or even the presence of minute amounts of some specific ions promote alterations in their cellular homeostasis, giving rise to severe human diseases including cancer, diabetes, and neurodegenerative diseases.[1,2] Thus, rapid, sensible, and accurate quantification of these species in the environment and in an organism is essential to monitor and maintain adequate health levels. Further, the investigation of these species in living organisms at the cellular level is becoming an essential tool to understand the chemical biology of anions and cations and their connection with health and disease.[3]

For several decades, classical analytical chemistry was founded on systematic sequential identification of inorganic species with general reagents exploiting the chemical equilibrium.[4] Organic reagents were used to identify cations, anions, or even to speciate very similar inorganic chemical species based on the visual change (colorimetric) promoted by highly selective binding with target analytes.[5,6] Nowadays, the development of nanotechnology in its subfields of nanophotonics and plasmonics and their application to spectroscopy, especially in surface-enhanced Raman scattering (SERS) spectroscopy,[7,8] offers new opportunities for pushing forward these classical methods. In particular, incorporation of organic reagents in SERS-based devices is well suited for applications aimed at the detection of small inorganic molecules with small Raman cross-section and, often, poor affinity toward the metal surfaces. Under such restrictions, indirect SERS approaches are therefore preferred in ion sensing.[9] Indirect detection is usually achieved by monitoring the changes in the overall SERS intensity of a Raman reporter[9,10] or the alteration of the spectral profile that a chemoreceptor undergoes upon complexation with the target species.[9,11] Although other experimental techniques are able to detect inorganic cations and anions at ultralow levels (i.e., fluorescence, atomic absorption or emission spectroscopies, chromatography, mass spectrometry, or electrochemical methods), the optical sensors based on plasmonic nanoparticles,[12] such as those developed using SERS,[13,14] allow for the study of inorganic small compounds in living organisms[15,16] and with a multiplex ability.

A paradigmatic example of the possibility to combine classical colorimetric reactions with SERS to yield highly sensitive and selective sensors is represented by the Griess reaction for nitrite determination. Griess reaction was first described in 1879.[17] Because of its simplicity, it has been used extensively in the analysis of numerous natural or biological
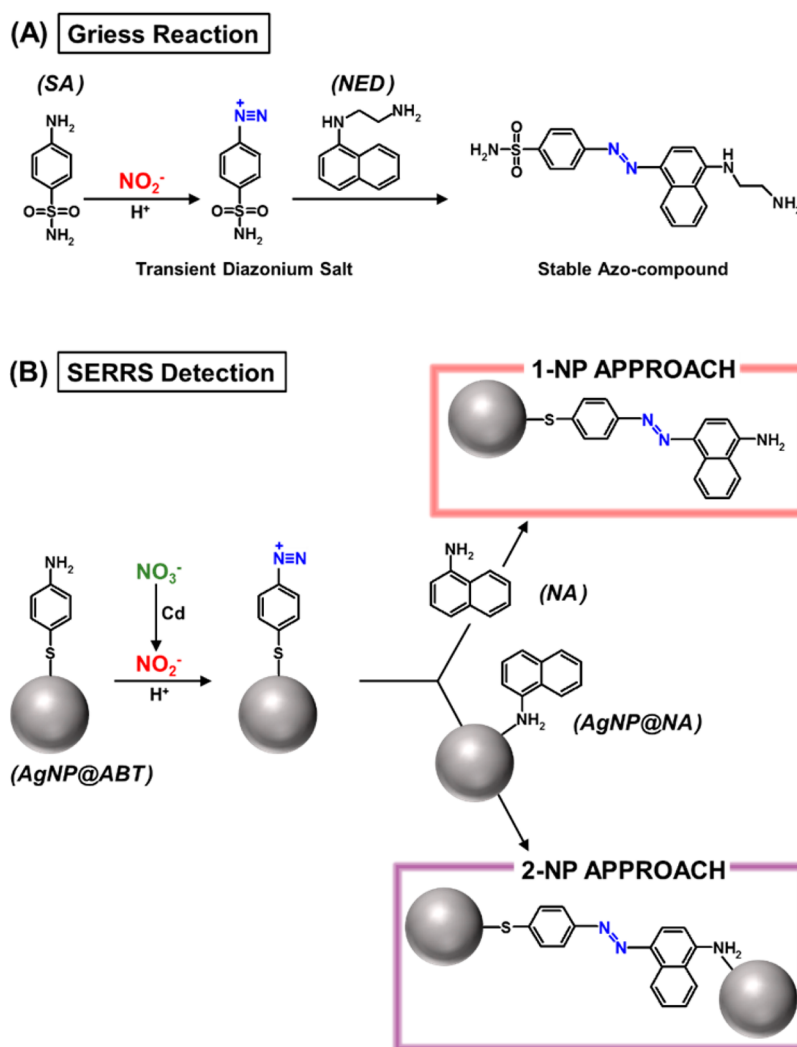
Figure 1. Schemes of the (A) colorimetric nitrite determination via the classical Griess reaction and (B) SERS/SERRS nitrite/nitrate determination using one nanoparticle or two nanoparticle strategies (1-NP approach and 2-NP approach, respectively).

samples including plasma, urine, or saliva.[18] In this method, nitrite is first treated in acidic media with a diazotizing reagent (sulfanilamide, SA) to form a transient diazonium salt. This intermediate is then allowed to react with a coupling reagent (*N*-naphthyl-ethylenediamine, NED) to form a stable azo-compound. The overall reaction is described in Figure 1A. The intense purple color of the product is the key for achieving a nitrite assay with high sensitivity that can be used to measure nitrite concentration as low as the ∼0.5 mM level. The absorbance of this adduct at 540 nm (Figure S1) is linearly proportional to the nitrite concentration in the sample. Although this reaction detects only nitrites, nitrates can also be analyzed by previously treating the sample with a reducing agent (such as cadmium, zinc, or hydrazine, or with enzymes such as the bacterial nitrate reductase) that converts NO_3^- into NO_2^-.

Recently, a few reports have described the engineering of SERS-platforms exploiting the selective formation of azo-compounds to detect nitrite anions in aqueous samples.[19−21] However, for different reasons, the proposed strategies were not devised to fully exploit the outstanding analytical potential of SERS as indicated by the relatively high detection limits

around the μM regime even when analyte accumulation schemes were employed.

In this Letter, we describe the rational design of a Griess-based SERS sensor for determination of nitrite and nitrate anions down to the subpicomolar regime. The illustrated optimization protocol builds on the main concepts of SERS and plasmonics to maximize the sensitivity of the sensor while preserving the selectivity and reproducibility required for reliable quantitative analysis. The outstanding performance of this new method is compared with those of the classical Griess reaction and ionic chromatography for a number of samples including tap and spring water and plasma.

Despite the increasingly huge number of novel SERS substrates fabricated in the past decade, gold and silver colloids prepared via wet chemical methods likely represented, and still are, the most widespread source of SERS substrates due to their simple and low-cost syntheses, ease of manipulation, and high SERS activity (especially when the individual nanoparticles are organized into "plasmonic molecules"[22]). Importantly, silver nanoparticles also show, contrary to gold nanostructures, high photonic efficiency in the green spectrum (i.e., the interband transition of silver is placed in the UV).[23,24] For these reasons, we selected silver nanoparticles (AgNPs) as optical enhancers.
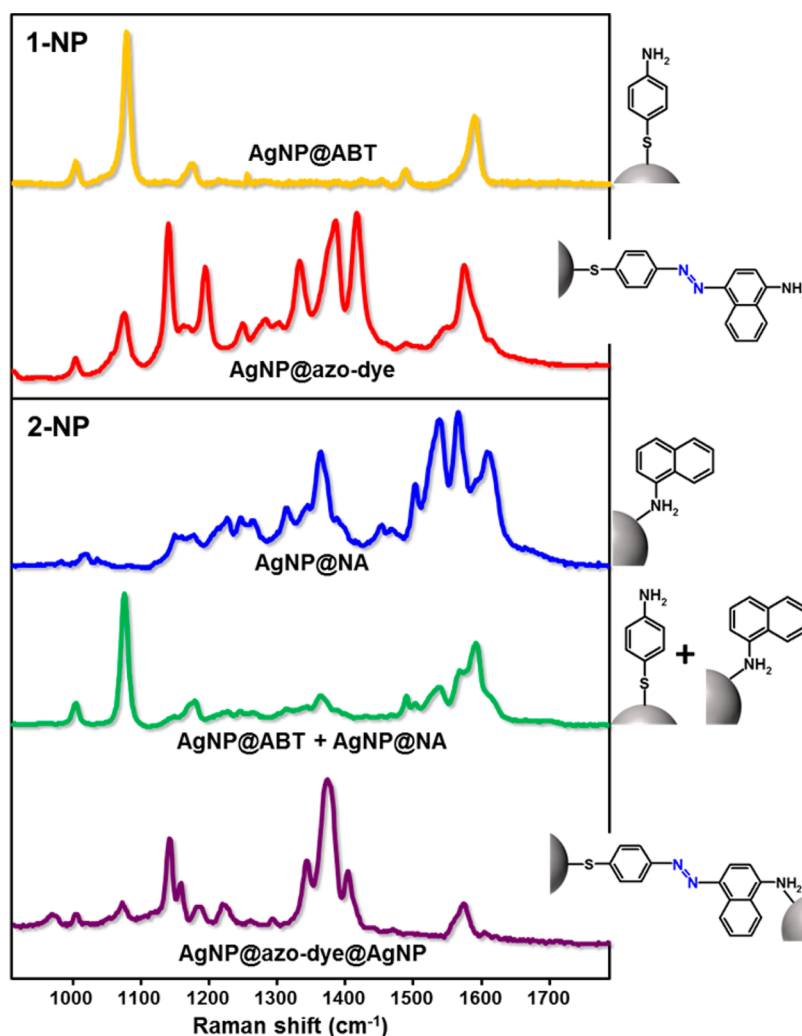
Figure 2. Normalized SERS and SERRS spectra of the following colloidal suspensions. 1-NP: AgNP@ABT (yellow curve) and AgNP@azo-dye (red curve). 2-NP: AgNP@NA (blue curve); colloidal mixture AgNP@NA + AgNP@ABT (2:1 molar ratio, green curve); and AgNP@azo-dye@AgNP (purple curve).

AgNPs were prepared through a hydrothermal method[25] yielding homogeneous spherical colloid with diameter around 30 nm. These materials present a narrow localized surface plasmon resonance (LSPR) with a maximum at 412 nm. Second, the experiments were designed to obtain statistically averaged spectra from a relatively high number of scatterers and nanoparticles in continuous Brownian motions within the scattering volume (i.e., average-SERS), by using a long-working distance objective to focus the 514 nm laser onto the sample solution. The average-SERS regime usually offers high spectral reproducibility and stability, as required for reliable quantitative analysis.[26] On the other hand, this analytical regime normally provides moderate enhancement factors (usually in the 10^4–10^7 range).[26,27]

We therefore pursue an improvement of the SERS activity by maximizing each of the multiplicative contributions that define the overall SERS enhancement: the electromagnetic and chemical enhancements (EM and CM, respectively). The former is independent of the target molecule and relies on the large electromagnetic fields generated at the nanostructure surfaces when LSPRs are excited via interaction with incident light.[26,27] On the contrary, the latter mechanism is solely associated with the intrinsic Raman properties of the molecule under study (i.e., Raman cross-section).[26,27]

The design of an equivalent Griess reaction for SERS requires the reagents to be bound to plasmonic nanoparticles. Thus, in order to demonstrate the possibility of using SERS spectroscopy as the transductor, SA and NED reagents were substituted by 4-amino benzenethiol (ABT) and 1-naphthyl-amine (NA), respectively (Figure 1B).[28] ABT firmly attaches to the metal surface via formation of a strong silver–sulfur bond (AgNP@ABT), whereas NA adsorption relies on the high affinity of nitrogen atoms for silver (AgNP@NA). Figure 2 illustrates the SERS spectra of both ABT and NA on silver colloids. Importantly, as for SA, the ABT molecule forms a diazonium derivative in the presence of NO_2^- under acidic conditions, which rapidly reacts with NA to yield a red azo-compound, characterized by a broader absorption with a maximum at 512 nm (Figure S1).

Notably, ABT suffers from photocatalyzed diazotization to yield p,p′-dimercaptoazobenzene (DMAB) when it is attached to gold or silver nanoparticles (Supporting Information Figure S2A, intraparticle dimerization).[29,30] Clearly, this catalytic effect has a negative impact on the performance of our sensor because it hampers the interaction of ABT with the target analyte.

Additionally, ABT dimerization involving molecules bound to different nanostructures (interparticle dimerization) can lead to cluster formation and colloidal destabilization. The first issue (intraparticle dimerization) was addressed by progressively decreasing the surface coverage of ABT (see time-dependence of the SERS spectra of ABT at different concentrations in Figure S2B). The data indicate that, while keeping constant the nanoparticle concentration to 10^{-4} M in silver, a dilution of the added amount of ABT to 10^{-7} M (final concentration, equivalent to 1 molecule per 3.7 nm^2) does not reveal any dimerization features in the SERS spectrum even for a long time, suggesting that surface-bound ABT molecules are eventually located far enough from each other to prevent dimerization events. Thus, AgNP@ABT colloids employed in our sensing platform were designed according to these findings ([ABT] = 10^{-7} M and [Ag] = 10^{-4} M). See Supporting Information for a detailed discussion of the data. On the other hand, the problem associated with interparticle dimerization was overcome by diluting AgNP@ABT nanoparticles ([Ag] = 1 × 10^{-4} M) with AgNPs ([Ag] = 2 × 10^{-4}) in a 1:2 molar ratio (total silver content equals 3 × 10^{-4} M). Within these experimental conditions, no evidence of aggregation was observed under transmission electron microscopy (TEM) investigation.

With the previous data in mind, we envisioned two alternatives to test for the design of our sensing platform. In the first one (Figure 1B, 1-NP approach), nitrite solution was added to a mixture of AgNP@ABT and unfunctionalized AgNPs (molar ratio 1:2, final silver concentration = 3 × 10^{-4} M) at pH 3.5, followed by the addition of NA (final concentration 10^{-6} M). After waiting 10 min for the reaction to occur, samples were analyzed by SERS upon excitation with a 514 nm laser. The generation of the azo-complex is revealed by the appearance of a new spectrum (Figure 2) which differs from those of the individual reagents bound onto the silver nanoparticles (AgNP@ABT and AgNP@NA) and their mixture (AgNP@NA + AgNP@ABT). Notably, the laser excitation energy is in resonance with an electronic transition within the azo-compound (resonant Raman, RR) that further enhances the signal in between 2 and 5 orders of magnitude.[31] The combination of SERS and RR scattering is referred to as SERRS (surface-enhanced *resonant* Raman scattering) and is characterized by a drastic increase in sensitivity (i.e., maximization of the chemical enhancement contribution to the overall EF). Figure 3A shows the nitrite concentration dependence of the SERRS spectra using the 1-NP approach in the 1300−1460 cm^{-1} spectral range. The results were obtained investigating aqueous solutions of nitrite in the 10^{-4} to 10^{-9} M range. It is worthy of note that concentrated solutions should be diluted prior to the analysis, as our sensor saturates at 0.1 μM. Representation of the SERRS intensity as a function of nitrite concentration (logarithmic scale) shows a linear trend down to the nanomolar regime (Figure 3D, red dots and trace). These detection limits are 2 orders of magnitude lower than classical Griess method and in the same order of magnitude as some electrochemical methods and ionic chromatography.[32]

Building on the outcomes of this first detection strategy, we pursue a further improvement of the SERS sensitivity via an augment of the electromagnetic enhancement provided by the plasmonic substrate. In this regard, we profit from the plasmon coupling of interacting nanoparticles that localizes large local fields at the interparticle junction ("hot spot"), which may
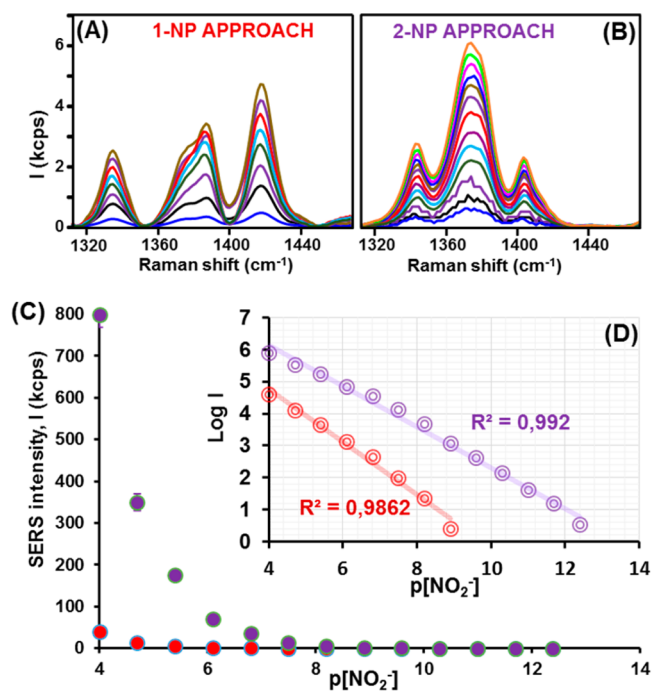
Figure 3. (A,B) Details of the 1310−1470 cm^{-1} spectral range for SERRS spectra of the diazo-complex at different nitrite concentrations for (A) 1-NP and (B) 2-NP approach. Bands can be assigned to ring and N═N stretchings (133 and 1386 cm^{-1}, and 1342 and 1373 cm^{-1} for the 1-NP and 2-NP approach, respectively) and C−H in plane bending (1417 and 1402 cm^{-1} for the 1-NP and 2-NP approach, respectively). (C,D) SERRS intensity of the N═N stretching as a function of the nitrite concentration for 1-NP approach (red dots) and 2-NP approach (purple) expressed both in (C) linear and (D) logarithmic scale. Error bars are equal to three standard deviations (N = 3).

exceed up to 10^3-10^5 times those observed on isolated nanoparticles.[27,31] To do so, a second batch of silver nanoparticles obtained by functionalizing the colloids with NA (AgNP@NA, where [NA] = 10^{-6} M and [Ag] = 10^{-4} M) was added to AgNP@ABT in a 2:1 molar ratio (final solution of 3 × 10^{-4} M in silver; Figure 1B, 2-NP approach). Addition of nitrite solutions at acidic pH promotes the formation of the azo-dye complex that acts as an interparticle cross-linker inducing the assembly of the nanoparticles into stable clusters in suspension, as revealed by the reshaping of the extinction profile (Figure 4). It is worth noting that the acquired SERRS spectrum shows a spectral profile similar to its analogue, the 1-NP approach (Figure 2) but with significant changes in relative intensities, which can be attributed to the surface selection rules.[33] The SERRS spectra obtained by addition of different nitrite amounts are illustrated in Figure 3B, whereas the corresponding signal intensities are plotted against the analyte concentration in Figure 3C,D, both in linear and logarithmic scales (purple dots and trace). The overall intensity obtained via the 2-NP approach far exceeds the previous results obtained with the 1-NP approach. The detection limits were dramatically improved down to the subpicomolar regime, in concrete until 4 × 10^{-13} M, consistently with the nitrite-driven formation of optical hot spots at the small interparticle gaps.[34,35]

The gap between molecularly aggregated colloids was calculated to be 1.31 nm by modeling the azo-compound with DFT methods (Figure 4).[13] The enhancing efficiency increases as the distance between the particle decreases and,
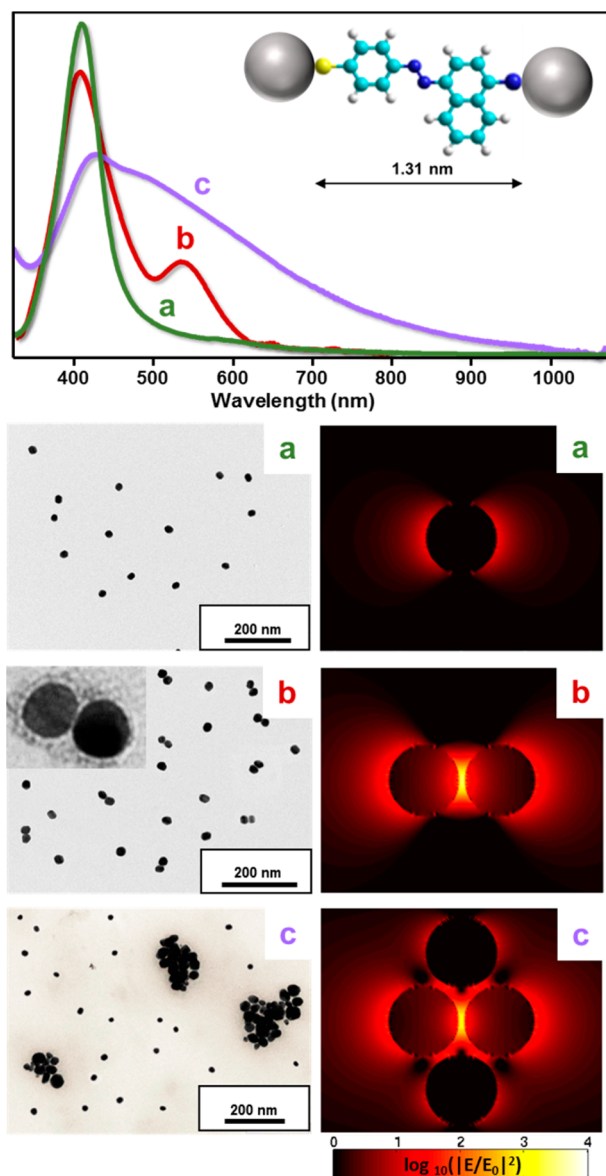
Figure 4. Extinction spectra, representative TEM images, and calculated electrical fields upon excitation with a 514 nm laser line for (a) AgNP@ABT in the presence of NO_2^- (10^{-7} M) and NA; and (b,c) mixture of AgNP@ABT and AgNP@NA (molar ratio 1:2) at 10^{-11} M (b) and 10^{-7} M (c) of NO_2^-.

especially, if it is smaller than 2 nm due to the appearance of the nonlocal effects (quantum confinement).[36,37] Remarkably, when the number of nitrite molecules is smaller than that of particles (nitrite concentration <10^{-10} M), a concentrated population of dimers is observed (Figure 4b). This image is consistent with the LSPR measured in these solutions (Figure 4b), which shows a second band at 540 nm, in addition to the dipolar LSPR of small single spheres, that can be attributed to the strong plasmonic coupling in dimers.[38] In contrast, at higher analyte concentrations, the LSPR broadens as a consequence of the multiparticle plasmonic interactions. This effect is also corroborated by TEM measurements (Figure 4c). To acquire deeper information about the magnitude of the electromagnetic fields generated at the hot spots, theoretical calculations were carried out for single particles, dimers and tetramers (this last one emulating the aggregate), considering

1.31 nm as the interparticle distance. The electromagnetic maps (Figure 4, right column) show a notable larger field (2 orders of magnitude) for the particles interacting versus those isolated giving rise to a rational explanation of the intensity increase in the 2-NP approach as compared with 1-NP.

Importantly, such outstanding SERS sensitivity was achieved while preserving high signal reproducibility, as indicated by the minimal variation of the signal from sample to sample (see standard deviations in Figure 3C). This can be ascribed to several factors, in addition to the acquisition of the spectra under the average-SERS regime. These include the assembly of the nanoparticles into stable clusters with well-defined interparticle distances fixed by the molecular length of the azo-complex. This largely limits possible gap-to-gap inhomogeneity that can significantly broaden the distribution of the EM enhancements at different hot spots. Furthermore, the nitrite concentration is directly correlated to the SERS intensity of the new surface azo-dye whose spectral fingerprint drastically differs from those of mechanical mixtures of AgNP@ABT and AgNP@NA colloids. Thus, the detected SERRS profile is solely related to the recognition event associated with the presence of the target analyte, avoiding reproducibility issues associated with a potential nanoparticle aggregation due to uncontrolled external factors.

There are a large number of methods for determining nitrate and nitrite ions, such as spectrophotometric (UV/vis, IR, fluorimetric) and electroanalytical,[32] but the most common detection strategies are, apart from the Griess-based protocols, ion chromatography (IC) and high-performance liquid chromatography (HPLC) combined with end column detection systems such as UV, fluorimetric, and conductometric systems.[39,40] In particular, IC has become a standard method[41] to apply in the identification and determination of nitrite and nitrate in all kinds of water samples, gases absorbed in solutions, food products, and biological samples.[39] Moreover, when combined with postcolumn derivatization methods, IC provided sensitivity down to the ca. 10^{-8} M regime of nitrate and nitrite.[40] Therefore, to test the applicability of our method, different samples were analyzed by using our sensing platform and compared with the results offered by the Griess reaction and IC (Figure 5). For our approach and the Griess reaction,
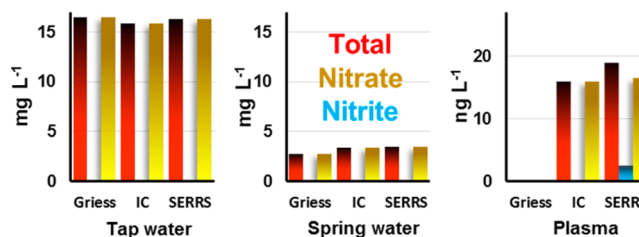

Figure 5. Performance comparison of the 2-NP approach with the classical Griess reaction and with IC for the analysis of nitrate/nitrite in tap water, spring water, and plasma.

two measurements were carried out. Each sample was divided into two aliquots: one was directly analyzed for the determination of nitrite, and the second was previously treated with a cadmium pellet in order to reduce the nitrate to nitrite and then analyzed. The three methods yield similar results with the water samples without any presence detected of nitrite. Regarding the plasma, the Griess reaction offers a negative result for both nitrite and nitrate, while IC and SERS show

similar results for nitrate. In the case of nitrite, the SERS method confirms the presence of a minute amount of nitrate that IC is not able to determine as it is out of its detection limit.

In summary, we have illustrated how to convert and optimize a classical sensing method into an ultrasensitive modern one by using concepts of nanophotonics, nanofabrication, and spectroscopy. The sensing method presented here exploits all the advantages of SERS/SERRS by (i) efficiently inducing the formation of a homogeneous hot spot during the diazotization reaction responsible for the analyte detection, and (ii) illuminating the sample with a laser line in resonance with the HOMO−LUMO levels of the so-formed colored complex. These two combined features allow for detection limits of about 6 orders of magnitude lower as compared with the classical Griess reaction and about 2−3 as compared with other instrumental alternatives such as IC. We hope this Letter paves the way for the development of new SERS devices exploiting the well-characterized old analytical chemistry for the monitoring of ionic inorganic species in a multiplex fashion in complex media, including living systems.

■ ASSOCIATED CONTENT

S Supporting Information

Experimental materials and methods; absorption and emission spectra of SA+NED and ABT+NA; time-dependence study of the ABT SERS spectra at different surface coverage. This material is available free of charge via the Internet at http://pubs.acs.org.

■ AUTHOR INFORMATION

Corresponding Authors
*E-mail: macorrea@uvigo.es.
*E-mail: ramon.alvarez@urv.cat.
Notes
The authors declare no competing financial interest.

■ ACKNOWLEDGMENTS

■ REFERENCES

(1) Finney, L. A.; O'Halloran, T. V. Transition Metal Speciation in the Cell: Insights from the Chemistry of Metal Ion Receptors. *Science* **2003**, *300*, 931−936.

(2) Domaille, D. W.; Que, E. L.; Chang, C. J. Synthetic Fluorescent Sensors for Studying the Cell Biology of Metals. *Nat. Chem. Biol.* **2008**, *4*, 168−175.

(3) Que, E. L.; Domaille, D. W.; Chang, C. J. Metals in Neurobiology: Probing Their Chemistry and Biology with Molecular Imaging. *Chem. Rev.* **2008**, *108*, 1517−1549.

(4) King, E. J. *Qualitative Analysis and Electrolytic Solutions*. Harcourt, Brace, and World: New York, 1959.

(5) Kolthoff, I. M. Application of Macrocyclic Compounds in Chemical Analysis. *Anal. Chem.* **1979**, *51*, 1R−22R.

(6) Feigl, F. Organic Reagents in Inorganic Analysis. *Indust. Eng. Chem. Anal. Ed.* **1936**, *8*, 401−410.

(7) Schlücker, S. Surface-Enhanced Raman Spectroscopy: Concepts and Chemical Applications. *Angew. Chem., Int. Ed.* **2014**, *53*, 4756−4795.

(8) Moskovits, M. Persistent Misconceptions Regarding SERS. *Phys. Chem. Chem. Phys.* **2013**, *15*, 5301−5311.

(9) Alvarez-Puebla, R. A.; Liz-Marzan, L. M. SERS Detection of Small Inorganic Molecules and Ions. *Angew. Chem., Int. Ed.* **2012**, *51*, 11214−11223.

(10) Krpetic, Z.; Guerrini, L.; Larmour, I. A.; Reglinski, J.; Faulds, K.; Graham, D. Importance of Metal−Adsorbate Interactions for the Surface-Enhanced Raman Scattering of Molecules Adsorbed on Plasmonic Nanoparticles. *Small* **2012**, *8*, 707−714.

(11) Guerrini, L.; Rodriguez-Loureiro, I.; Correa-Duarte, M. A.; Lee, Y. H.; Ling, X. Y.; Garcia de Abajo, F. J.; Alvarez-Puebla, R. A. Chemical Speciation of Heavy Metals by Surface-Enhanced Raman Scattering Spectroscopy: Identification and Quantification of Inorganic- and Methyl-Mercury in Water. *Nanoscale* **2014**, *6*, 8368−8375.

(12) Jimenez de Aberasturi, D.; Montenegro, J.-M.; Ruiz de Larramendi, I.; Rojo, T.; Klar, T. A.; Alvarez-Puebla, R.; Liz-Marzán, L. M.; Parak, W. J. Optical Sensing of Small Ions with Colloidal Nanoparticles. *Chem. Mater.* **2012**, *24*, 738−745.

(13) Tsoutsi, D.; Montenegro, J. M.; Dommershausen, F.; Koert, U.; Liz-Marzán, L. M.; Parak, W. J.; Alvarez-Puebla, R. A. Quantitative Surface-Enhanced Raman Scattering Ultradetection of Atomic Inorganic Ions: The Case of Chloride. *ACS Nano* **2011**, *5*, 7539−7546.

(14) Moskovits, M. Surface-Enhanced Spectroscopy. *Rev. Mod. Phys.* **1985**, *57*, 783−826.

(15) Rivera_Gil, P.; Vazquez-Vazquez, C.; Giannini, V.; Callao, M. P.; Parak, W. J.; Correa-Duarte, M. A.; Alvarez-Puebla, R. A. Plasmonic Nanoprobes for Real-Time Optical Monitoring of Nitric Oxide inside Living Cells. *Angew. Chem., Int. Ed.* **2013**, *52*, 13694−13698.

(16) Ravindranath, S. P.; Henne, K. L.; Thompson, D. K.; Irudayaraj, J. Raman Chemical Imaging of Chromate Reduction Sites in a Single Bacterium Using Intracellularly Grown Gold Nanoislands. *ACS Nano* **2011**, *5*, 4729−4736.

(17) Griess, P. *Ber. Deutsch Chem. Ges.* **1879**, *12*, 426−428.

(18) Casey, T. E.; Hilderman, R. H. Modification of the Cadmium Reduction Assay for Detection of Nitrite Production Using Fluorescence Indicator 2,3-Diaminonaphthalene. *Nitric Oxide* **2000**, *4*, 67−74.

(19) Kim, K.; Kim, K. L.; Shin, K. S. Selective Detection of Aqueous Nitrite Ions by Surface-Enhanced Raman Scattering of 4-Aminobenzenethiol on Au. *Analyst* **2012**, *137*, 3836−3840.

(20) Ma, P.; Liang, F.; Li, X.; Yang, Q.; Wang, D.; Song, D.; Gao, D.; Wang, X. Development and Optimization of a SERS Method for on-Site Determination of Nitrite in Foods and Water. *Food Anal. Methods* **2014**, *7*, 1866−1873.

(21) Zhang, K.; Hu, Y.; Li, G. Diazotization-Coupling Reaction-Based Selective Determination of Nitrite in Complex Samples Using Shell-Isolated Nanoparticle-Enhanced Raman Spectroscopy. *Talanta* **2013**, *116*, 712−718.

(22) Halas, N. J.; Lal, S.; Chang, W.-S.; Link, S.; Nordlander, P. Plasmons in Strongly Coupled Metallic Nanostructures. *Chem. Rev.* **2011**, *111*, 3913−3961.

(23) Abalde-Cela, S.; Ho, S.; Rodríguez-González, B.; Correa-Duarte, M. A.; Álvarez-Puebla, R. A.; Liz-Marzán, L. M.; Kotov, N. A. Loading of Exponentially Grown LbL Films with Silver Nanoparticles and Their Application to Generalized SERS Detection. *Angew. Chem., Int. Ed.* **2009**, *48*, 5326−5329.

(24) Zhao, J.; Pinchuk, A. O.; McMahon, J. M.; Li, S.; Ausman, L. K.; Atkinson, A. L.; Schatz, G. C. Methods for Describing the Electromagnetic Properties of Silver and Gold Nanoparticles. *Acc. Chem. Res.* **2008**, *41*, 1710−1720.

(25) Yu, D.; Yam, V. W.-W. Hydrothermal-Induced Assembly of Colloidal Silver Spheres into Various Nanoparticles on the Basis of HTAB-Modified Silver Mirror Reaction. *J. Phys. Chem. B* **2005**, *109*, 5497−5503.

(26) Aroca, R. *Surface-Enhanced Vibrational Spectroscopy*; John Wiley & Sons: Chichester, U.K., 2006.

(27) Le Ru, E. C.; Etchegoin, P. G. *Principles of Surface-Enhanced Raman Spectroscopy*; Elsevier: Amsterdam, 2009.

(28) Han, X. X.; Chen, L.; Kuhlmann, U.; Schulz, C.; Weidinger, I. M.; Hildebrandt, P. Magnetic Titanium Dioxide Nanocomposites for Surface-Enhanced Resonance Raman Spectroscopic Determination and Degradation of Toxic Anilines and Phenols. *Angew. Chem., Int. Ed.* **2014**, *53*, 2481−2484.

(29) Canpean, V.; Astilean, S. Temperature Effect on the SERS Signature of P-Aminothiophenol: A New Evidence for the Production of p,p′-Dimercaptoazobenzene on Metallic Nanostructures. *Spectrochim. Acta, Part A* **2012**, *96*, 862−867.

(30) Gabudean, A. M.; Biro, D.; Astilean, S. Localized Surface Plasmon Resonance (LSPR) and Surface-Enhanced Raman Scattering (SERS) Studies of 4-Aminothiophenol Adsorption on Gold Nanorods. *J. Mol. Struct.* **2011**, *993*, 420−424.

(31) Alvarez-Puebla, R. A. Effects of the Excitation Wavelength on the SERS Spectrum. *J. Phys. Chem. Lett.* **2012**, *3*, 857−866.

(32) Moorcroft, M. J.; Davis, J.; Compton, R. G. Detection and Determination of Nitrate and Nitrite: A Review. *Talanta* **2001**, *54*, 785−803.

(33) Moskovits, M.; DiLella, D. P.; Maynard, K. J. Surface Raman Spectroscopy of a Number of Cyclic Aromatic Molecules Adsorbed on Silver: Selection Rules and Molecular Reorientation. *Langmuir* **1988**, *4*, 67−76.

(34) Laurence, T. A.; Braun, G.; Talley, C.; Schwartzberg, A.; Moskovits, M.; Reich, N.; Huser, T. Rapid, Solution-Based Characterization of Optimized SERS Nanoparticle Substrates. *J. Am. Chem. Soc.* **2008**, *131*, 162−169.

(35) Camden, J. P.; Dieringer, J. A.; Wang, Y.; Masiello, D. J.; Marks, L. D.; Schatz, G. C.; Van Duyne, R. P. Probing the Structure of Single-Molecule Surface-Enhanced Raman Scattering Hot Spots. *J. Am. Chem. Soc.* **2008**, *130*, 12616−12617.

(36) García de Abajo, F. J. Light Scattering by Particle and Hole Arrays. *Rev. Mod. Phys.* **2007**, *79*, 1267−1290.

(37) Alvarez-Puebla, R.; Liz-Marzán, L. M.; García de Abajo, F. J. Light Concentration at the Nanometer Scale. *J. Phys. Chem. Lett.* **2010**, *1*, 2428−2434.

(38) Chen, G.; Wang, Y.; Yang, M.; Xu, J.; Goh, S. J.; Pan, M.; Chen, H. Measuring Ensemble-Averaged Surface-Enhanced Raman Scattering in the Hotspots of Colloidal Nanoparticle Dimers and Trimers. *J. Am. Chem. Soc.* **2010**, *132*, 3644−3645.

(39) Michalski, R.; Kurzyca, I. Determination of Nitrogen Species (Nitrate, Nitrite and Ammonia Ions) in Environmental Samples by Ion Chromatography. *Polym. J. Environ. Stud.* **2006**, *15*, 5−18.

(40) Nakatani, N.; Kozaki, D.; Mori, M.; Tanaka, K. Recent Progress and Applications of Ion-Exclusion/Ion-Exchange Chromatography for Simultaneous Determination of Inorganic Anions and Cations. *Anal. Sci.* **2012**, *28*, 845−852.

(41) Rice, E.W.; Baird, R.B.; Eaton, A.D.; Clesceri, L. S. *Standard Methods for the Examination of Water and Wastewater*, 22nd ed.; American Public Health Association, American Water Works Association, Water Environment Federation: Baltimore, MD, 2012.